



Journal Homepage: -[www.journalijar.com](http://www.journalijar.com)

## INTERNATIONAL JOURNAL OF ADVANCED RESEARCH (IJAR)

Article DOI:10.21474/IJAR01/16873  
DOI URL: <http://dx.doi.org/10.21474/IJAR01/16873>



### RESEARCH ARTICLE

#### STUDY OF KINETIC, ISOTHERMAL, AND SORPTION CHARACTERISTICS OF SOME DYES USING NOVEL LUPINE PEEL POWDER

Nada Mohamed Sayed<sup>1</sup>, Gamalat Al-Mohamady<sup>2</sup>, Samia Al-Hosainy Abo-Farha<sup>3</sup>, Nagwa Abdul Fattah Badawy<sup>4</sup> and Mohamed OsamaEl-Moatasem<sup>5</sup>

1. Research Assistant, Faculty of Science, Al-Azhar University (Girls Branch), Cairo, Egypt.
2. Assistant Prof. of Physical Chemistry, Faculty of Science, Al-Azhar University (Girls Branch), Cairo, Egypt.
3. Vice-dean for Education and Student Affairs, Faculty of Science, Al-Azhar Un. (Girls Branch), Cairo, Egypt.
4. Prof. of Physical Chemistry, Faculty of Science, Al-Azhar University (Girls Branch), Cairo, Egypt.
5. Prof. of Soil Chemistry, Faculty of Agriculture, Al-Azhar University (Male Branch), Cairo, Egypt.

#### Manuscript Info

##### Manuscript History

Received: 10 March 2023  
Final Accepted: 14 April 2023  
Published: May 2023

##### Key words:-

Wastewater, Basic Fuchsin, Eosin, Lupine Peel, Kinetics, Isotherms, Thermodynamics

#### Abstract

Synthetic dyes are considered harmful compounds to the environment even in slight quantities. Low-cost natural adsorbents have been proven helpful for water treatment. In the current research, Lupine peel was used in inactivated (IL) and activated (AL) forms to remove Basic Fuchsin (BF) and Eosin (E) dyes from aqueous media. Adsorbents have been evaluated by FTIR and SEM. The operational settings, including the solution's pH, adsorbent dosage & size, initial dye concentration, temperature & contact time were all controlled in a batch system. According to experimental outcomes, the adsorption procedure occurs quickly & naturally. A pseudo-2<sup>nd</sup>-order kinetic model gives the best fit to the experimental information of BF & E dyes adsorption onto IL and AL. Adsorption isotherm data of BF adsorption was fitted well to the Freundlich model, while E adsorption was well fitted to the Langmuir adsorption isotherm. Optimal adsorption capacities of 1.5344, 2.9913, 0.7983, and 1.0921 mg/g for BF and E adsorption onto IL and AL respectively. According to the (D-R) isotherm model, the values of E were 0.5, 2.357, 0.05, and 0.0707 KJ/mol for BF and E onto IL and AL respectively, indicating a physisorption process. The activation parameters ( $\Delta G^\circ$ ,  $\Delta H^\circ$ ,  $\Delta S^\circ$ ) were calculated. The adsorption was endothermic and spontaneous with a higher preference of BF than E onto AL and IL. The findings indicate that the lupine peel has the potential to function as a low-cost adsorbent for the elimination of BF & E dyes from aqueous solutions.

Copy Right, IJAR, 2023,. All rights reserved.

#### Introduction:-

Our world is facing the problem of water pollution due to the various industries. Synthetic materials can reach water bodies through factory drainage. These pollutants include dyes, which are extensively used in industries such as paper, paint, textiles, etc. [1]. Compared to organic pigments, the world produces large quantities of industrial pigments because of the ease of manufacture. The basic and acidic dyes are widely used in industry, so it is important to find a way to remove them from waterbodies or this will affect human health and the environment [2].

**Corresponding Author:- Nada Mohamed Sayed**

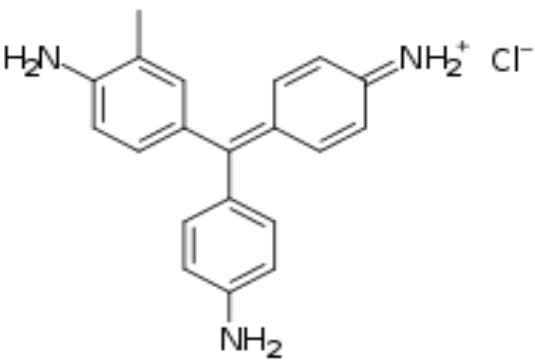
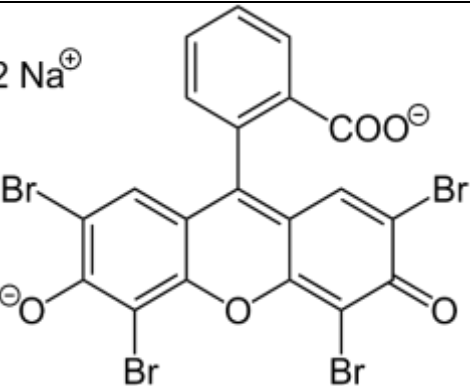
Address:- Research Assistant, Faculty of Science, Al-Azhar University (Girls Branch), Cairo, Egypt.

The released dyes into the water bodies as wastewater stains water, reduce the absorption of light by aquatic organisms, it is also considered toxic to human and living organisms. The conventional biological oxidation process cannot remove dye from wastewater Because of its slow biodegradability [1]. Basic Fuchsin is also known as Basic Violet 14; its chemical structure is represented in Table 1 [3]. It is one of the naturally inflammable triaryl methane dyes. It is anesthetic, fungicidal & bactericidal properties. It is utilized in numerous industries as a dye for textiles and leather, as well as for the staining of muscle, collagen & mitochondria. It is also poorly biodegradable, carcinogenic, and unattractive. Therefore, the elimination of Basic Fuchsin from wastewater systems is crucial. [4].

Eosin is also known as Acid Red 87; its chemical structure is represented in Table 1 [5]. It is used in the textile, art industry, and pharmaceutical processes [5]. It forms a water-soluble stable complex through binding with protein. According to this, it is also used in histology to stain cytoplasm. It is stable against degradation as a result of having an aromatic ring structure. It is considered a carcinogenic substance which causes destruction to the liver, kidneys, and lungs [6]. Its presence in high concentration can affect the central nervous system [7].

There are so many wastewater treatment techniques. Adsorption is very popular among researchers because it is a simple operation, we can use many kinds of adsorbent materials, it gives high removal results, and using natural products in the process makes it a low-cost one [1]. Lupine (*Lupinus termis* L.) is grown under a variety of circumstances in Egypt. Lupine has been cultivated for thousands of years. Its seed can be used as food because it contains protein and oil. In fact, for thousands of years, Egyptians have been benefiting from the therapeutic and nutritional properties of lupine seeds [8]. Therefore, using its peel in wastewater treatment will be the use of cheap local waste to conserve water. In this study, the lupine peel will be used as an adsorbent for Basic Fuchsin and Eosin dyes from aqueous solutions and its adsorption efficiency will be enhanced by the physicochemical activation process [9].

**Table 1:-** Dyes chemical structures and basic information.

Dye	IUPAC name	Chemical formula	Mol.wt g/mol	$\lambda_{\max}$ nm
Basic Fuchsin	benzenamine, 4-[(4-aminophenyl) (4-imino-2, 5-cyclohexadien-1-ylidene) methyl]-2-methyl hydrochloride		337.86	546
Eosin	disodium; 2-(2,4,5,7-tetrabromo-3-oxido-6-oxoxanthen-9-yl) benzoate		691.85	514

## Materials and Methods:-

Lupine seed can be obtained as a local Egyptian product, then its peel waste is used as an adsorbent with and without activation. Basic Fuchsin (BF) and Eosin (E) dyes were purchased from Maktab Al-Sharq, Qasr El-Ainy, Qairo, Egypt, and originally made in India (Advent, Chembio PVT.LTD company). The hydrochloric acid (HCl) as well as sodium hydroxide (NaOH) used in the experiment were likewise acquired from Maktab Al-Sharq.

Fourier Transform Infrared Spectroscopy (FTIR) & Scanning Electron Microscope (SEM) analyses were utilized to identify the functional groups and the morphological properties in the adsorbents IALP and ALP [10,11]. UV-VIS spectrophotometer was used to determine the dye concentrations through the batch adsorption experiments.

### Preparation of adsorbent

The adsorbents made from used lupine peels were rinsed thoroughly with distilled water until all traces of dirt and dust were eliminated. After air drying at room temperature the clean lupine peels, they were baked at 378K until they reached a steady weight. Then we have crushed the dried sample to obtain the untreated lupine peel adsorbent. To obtain the physicochemical activated lupine peels, half of the untreated lupine peel powder entered the oven at 573K for 4 hours (physical activation) to change porosity which, accordingly, increases adsorption efficiency. After cooling naturally, the physically activated lupine peels then were saturated with 1N NaOH with the ratio of 1:5 adsorbent wt. /NaOH volume for 4 hours (chemical activation). After being filtered, the activated adsorbent cleaned multiple times with distilled water to restore the solution's natural pH and then dried at 375K for twenty-four hours. Both activated & inactivated lupine peels adsorbent were crushed into 0.1mm and 0.2mm mesh sizes [9].

### Batch Adsorption Experiments

Various parameters, such as pH (3-11), adsorbent dosage (0.4-2 g), first dye concentration (35-335mg/l), contact time (5-180 min), temperature (298 K-343 K) and particle size (0.1mm, 0.2mm), were determined in batch mode adsorption tests. Dye solutions were neutralized with 1M NaOH or 1M HCl to achieve the desired pH levels.

The removal of dyes by both inactive and activated adsorbents is shown in the following equations (1) and (2), respectively [12].

$$\text{Removal efficiency (\%)} = (C_o - C_e / C_o) \times 100 \quad [1]$$

$$q_e (\text{mg /g}) = ((C_o - C_e) \times V) / m \quad [2]$$

Where  $C_o$  (mg/L) is the first concentration of basic fuchsin dye,  $C_e$  (mg/L) is liquid-phase concentrations of the basic fuchsin dye at balance,  $V$  (L) is the volume of the basic fuchsin dye &  $m$  (g) is the adsorbent mass [13,14].

## Result and Discussion:-

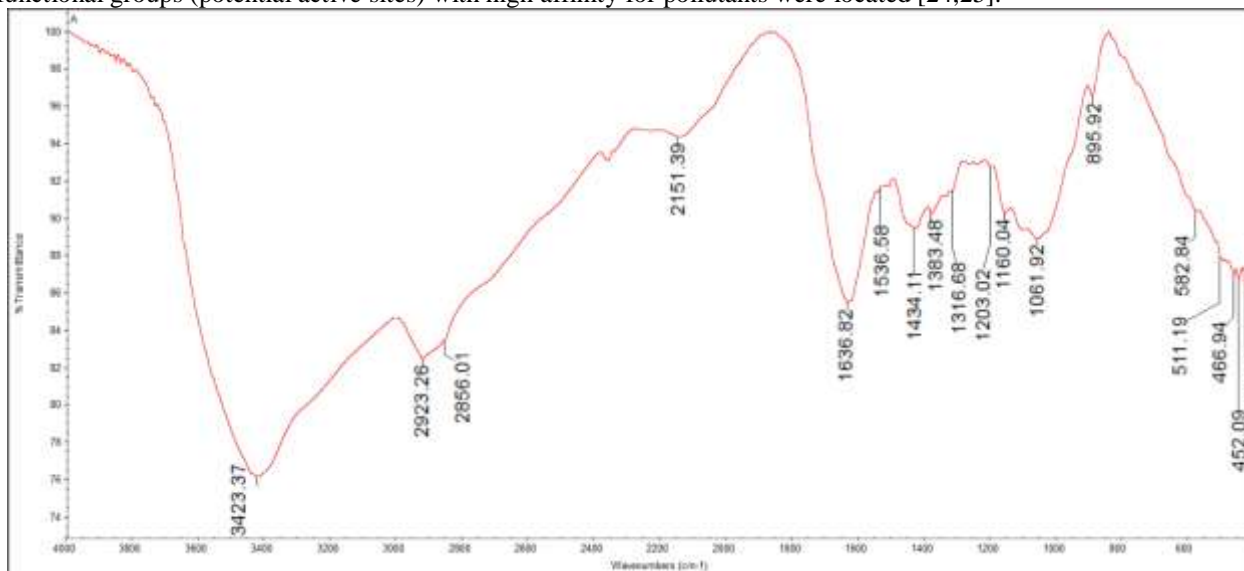
### Characterization of Lupine Peel Waste Adsorbents

Adsorbents' physicochemical properties was studied by FTIR and SEM analysis. The results indicate that the physicochemical activation removes most of the wetness & heat-sensitive molecules from the samples. The physicochemical activation causes fewer stability and releases the evaporable gas and liquid components of the volatile substance, so the organic components present in activated lupine peel adsorbent deteriorate in stability & the volatile matter becomes low [15]. Also, the activation process produces an adsorbent with a low ash content because of the removal of most mineral components such as oxides, carbonates and sulphides [9]. A constant amount of carbon of the activated lupine peel was great, which increases the quality of the adsorbent substance via enhancing the surface area which resulting in a higher adsorption efficiency [16].

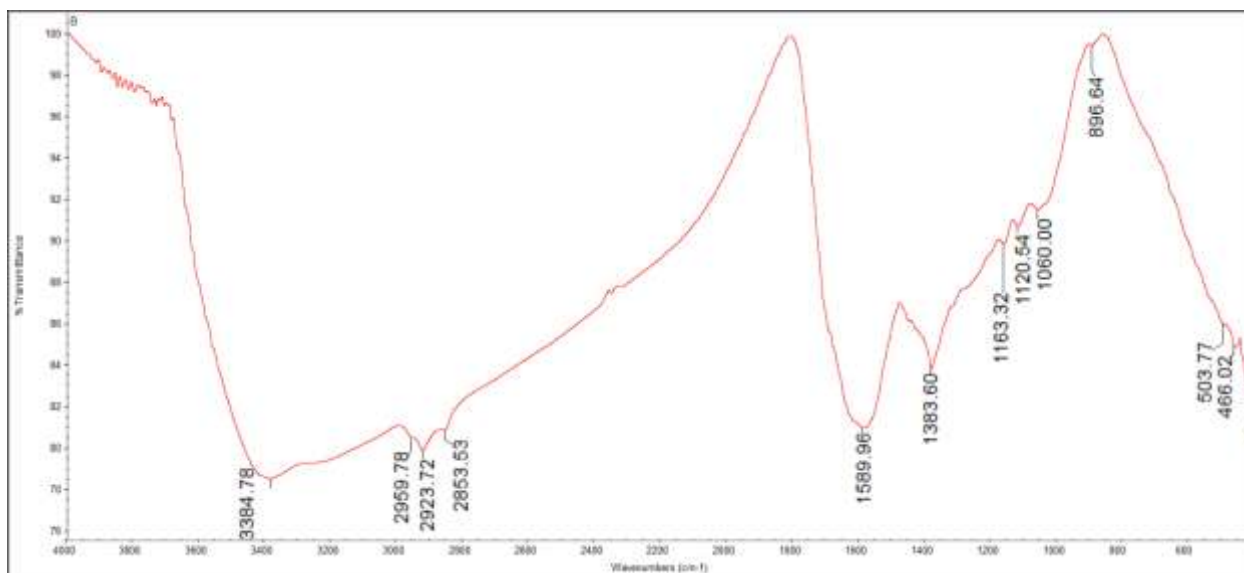
### Fourier Transformer Infrared

The FTIR spectra of IL, AL, AL loaded BF and AL loaded E dyes were studied between 4000 - 400  $\text{cm}^{-1}$ ; determined in Figure 1. Spectra (before & after adsorption), the broad & intense absorption peaks among 3423.37 for IL - 3384.78  $\text{cm}^{-1}$  for AL gained because of the hydroxyl (-O-H) or amine (-N-H) functional groups [17,18,19], the absorption peaks at 2923.26, 2856.1 for IL and 2959.78, 2923.72 and 2853.33  $\text{cm}^{-1}$  for AL can be redirected to the -C-H group of alkanes, stretching. The vibration at 2151.39 and 1636.82  $\text{cm}^{-1}$  for IL assigned to  $\text{C} \equiv \text{C}$  &  $\text{C} \equiv \text{N}$  - H bonds which disappears at AL spectrum [20,21], the peaks at 1434.11 and 1383.60  $\text{cm}^{-1}$  for IL and AL respectively are hypothetical to the existence of (OH) vibration of carboxylic acid and absorption bands from 1420 to 1000  $\text{cm}^{-1}$  can be apportioned to the C-O and C-N stretching vibration of carboxylic acids (-COOH) and/or

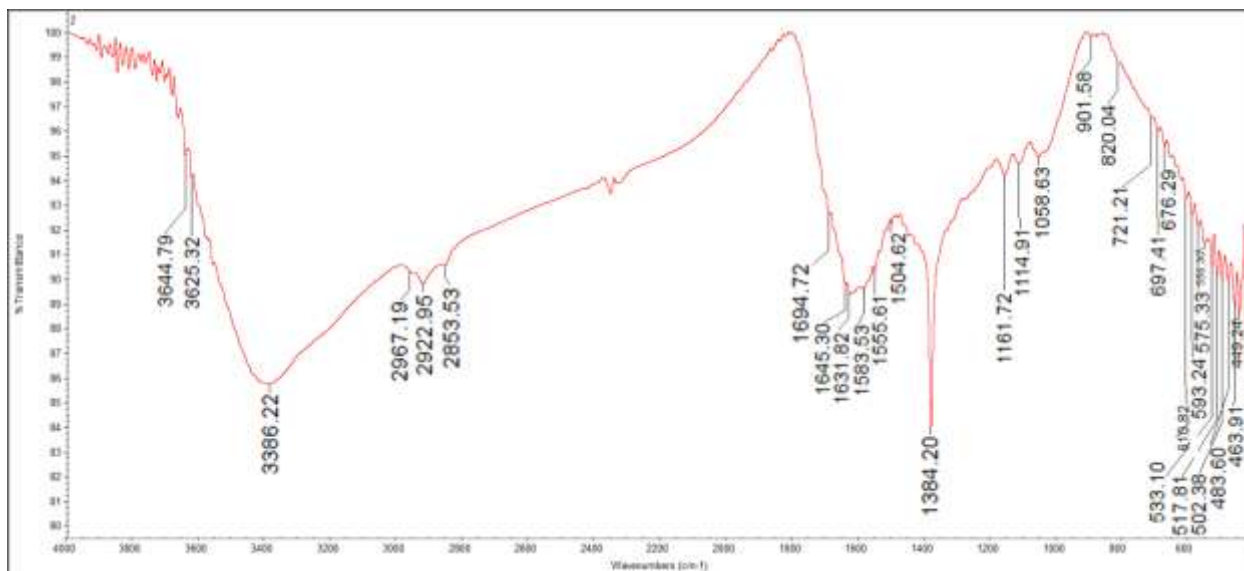
alcohols & amine groups [18,22]. The surface/characteristic peaks of IL & AL were originate to be changed (Figure 1) Some functional groups were chemically protonated/deprotonated & thermally unstable, as evidenced by their disappearance and changes in peak intensity during the physicochemical activation process [9,23]. Adsorption zones in the spectra of AL-loaded BF with AL-loaded E dyes were quite close to one another, with only minor variations. The Fourier transform infrared spectrum taken before and after adsorption show that the peaks move somewhat and the intensity changes. Based on these findings, it appears that hydroxyl, carbonyl, amine and carboxyl functional groups bond during adsorption via a weak electrostatic contact or Van der Waals forces [20,22]. Hydrogen bonding, electrostatic and  $\pi$ - $\pi$  interactions were responsible for the removal of both dyes from the IL and AL surfaces, where functional groups (potential active sites) with high affinity for pollutants were located [24,25].



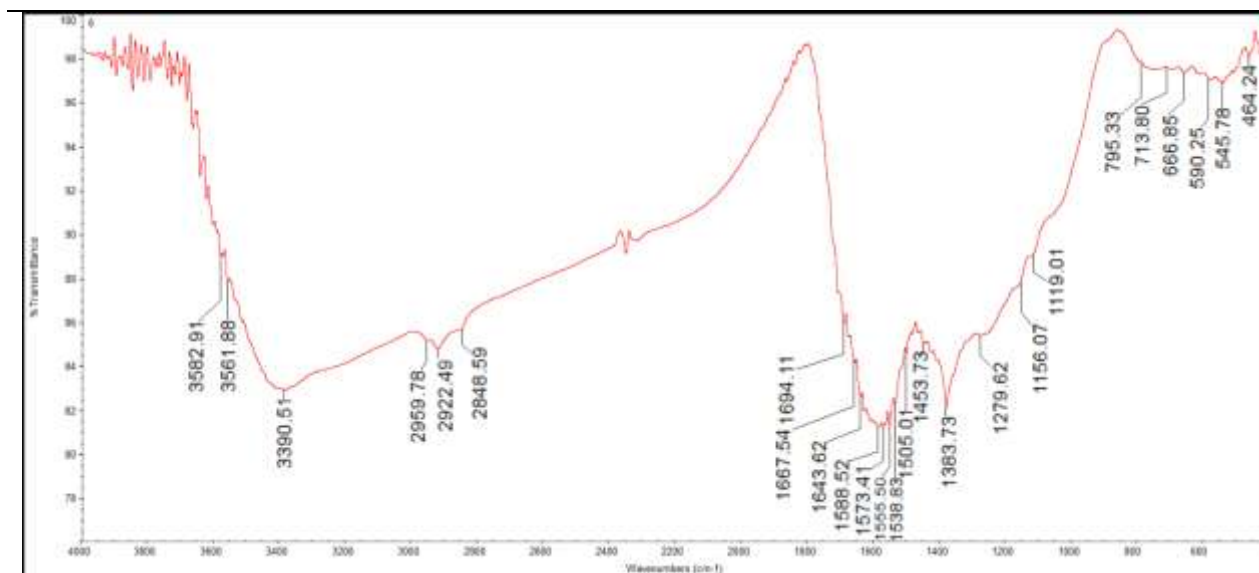
(a) FTIR spectrum of IL



(b) FTIR spectrum of AL



(c) FTIR spectrum of BF onto AL



(d) FTIR spectrum of E onto AL

**Fig. 1:-** FTIR spectrum.

### Scan Electron Microscope

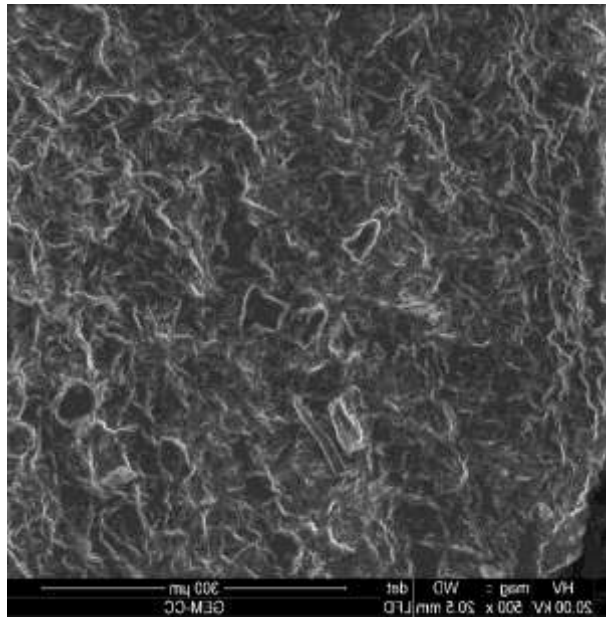
The SEM analysis was made before activation, after activation and after adsorption. The adsorbents surfaces are loaded and the dyes molecules occupied the surface pores. After the physical- chemical activation the pore size distribution of lupine peel increases and therefore the adsorption potential [26].

According to the activation, the NaOH molecules occupied the active sites after activation and changed the original surface texture of lupine peel, this enhanced the adsorbent physical characteristics.

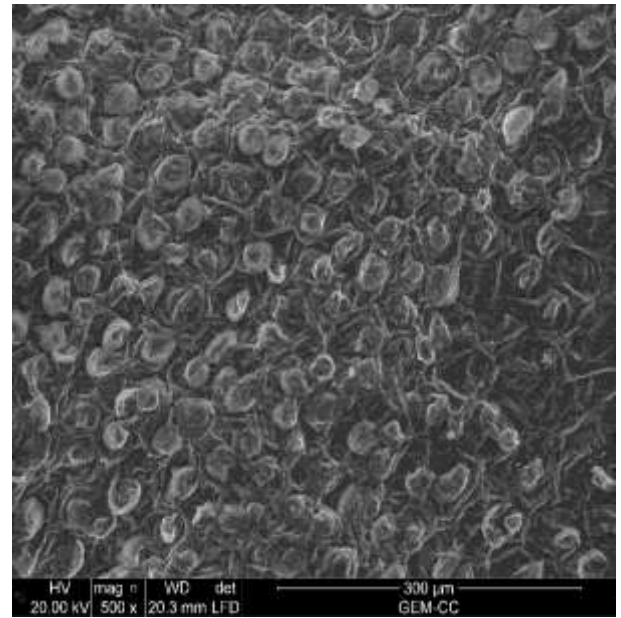
Through studying the images, the active sites of lupine peel were rough and random. The activation then, provides a regular shape of the active sites which look as spherical particles distributed orderly on the surface. The activated surface then, has cracks, grooves and large pores. This gives an evidence about the enhancement achieved by activation. These pores provided a good surface for dyes, to be confined & adsorbed into [15,27].

The NaOH gives negative charges for the active sites. These negatively charged active sites electrostatically attracted to the positive Basic Fuch sine more than Eosin dye. After adsorption of Basic Fuch sine, the enhanced active sites (look like tubes or cylinders) look completely full. These cylindrical shapes are methodically occupied by the basic dye molecules which favor the negatively charged surface.

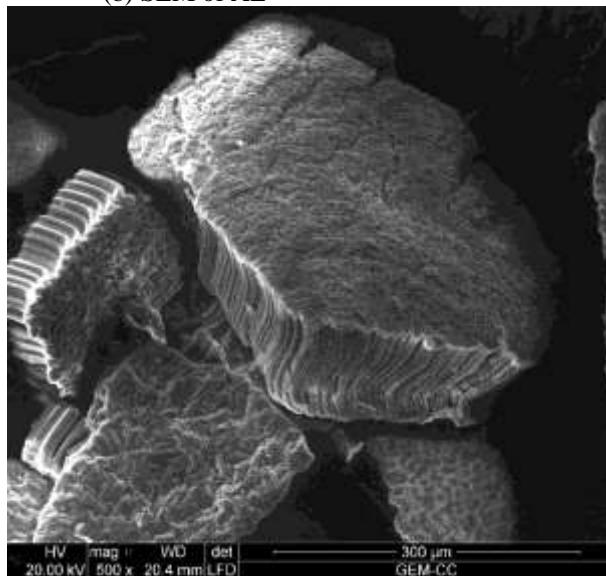
And yet, the enhanced active sites were occupied by the acidic dye molecules of Eosin dye, but not as the same vigorous occupation occurred by Basic Fuch sine dye.



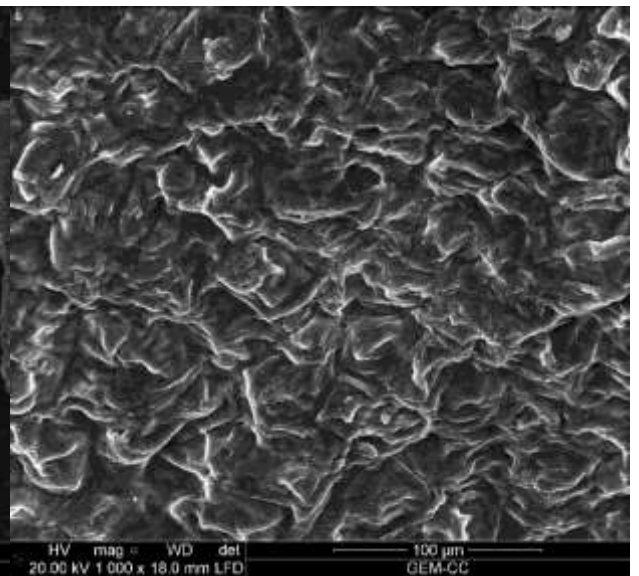
(b) SEM of AL



(a) SEM of IL



(c) SEM of AL-loaded BF



(d) SEM of AL-loaded E

Fig. 2:- SEM micrographs.

## Batch Adsorption Study

### Effect of Solution pH

Solution pH and Its Impact is a very relevant factor in adsorption experiments. In this trial, the adsorption studies of BF and E dyes on IL and AL were carried out at different pH values (3-11). The outcomes are shown in Figure 3. According to the Figure, the adsorption process of BF prefers the alkaline medium and removal increase with increasing pH to give higher removal at  $pH_{11}$  for both inactivated and activated adsorbents at affixed concentration.

In highly acidic solutions, the surface of the adsorbents (activated and inactivated lupine peel) become positively charged & they participate with a cationic basic fuchsin dye for vacant adsorption sites, resulting in a reduction in dye adsorption due to electrostatic repulsion.

The electrostatic force of attraction among the cationic basic fuchsin dye and the negatively charged adsorbent surface rises with increasing pH [9]. Physicochemical activation of the adsorbents resulted in a rise in the number of acidic functional groups (C=O, O-H and C-), as seen by the FT-IR study (Figure 5). Adsorption can take place among the cationic BF dye and the adsorbents via the adsorbents' acidic active surface. The high removal efficiency at higher  $pH_{11}$  value is maybe due to hydrogen bonding,  $\pi$ - $\pi$  interaction, or electrostatic attraction among adsorbent and adsorbate [17]. Furthermore, because of the significant surface area present, the process accountable for the adsorption of BF could be further closely associated with textural features [9]. Thus, the most effective BF elimination of dye occurred in basic regions (pH 11). On the other hand, at  $pH_3$  the surfaces of IALP and ALP were positively charged and more protons will be available to protonate amine groups and this increases the active positions and thus prefer anion sorption resulting in increasing the adsorption of E dye [28].

### Influence of Adsorbent Dose

The adsorbent dose is a very critical factor because it effects on the adsorbent & adsorbate [29]. The influence of adsorbent dose on the elimination of BF and E dyes onto IL and AL are shown in Figure 4. When the adsorbent's doses were enlarged from (0.4 to 2g), an increase in BF dye removal from 76.3 to 90.14% onto AL, and from 35.47 to 86.56% onto IL was observed. On the other hand, the removal of E onto IL was increased from 12.78 to 19.44%, while its removal onto AL was increased from 18.57 to 25.44%. This rise in dye removal with adsorbent dosage is caused by the adsorbents' expanding surface area and the availability of many adsorption sites [30]. Because of conglomeration/aggregation of adsorbent particles that limits the active surfaces for adsorption, at higher adsorbent doses (more than 1g for activated and inactivated adsorbents respectively) the dye removal was not significantly different or impacted [31].

### Influence of adsorbent particle size

The impact of adsorbent particle size on the adsorption processes was studied at 2 particle sizes (7mm & 8mm mesh size) at optimum values of  $pH_{11}$  for BF,  $pH_3$  for E, initial dye concentration 35 mg/L, adsorbents doses 2g, contact time thirty minutes & temperature 298K with an agitation speed of 200 rpm. As shown in Figure 5, the elimination of dyes rises with the decrease of adsorbent particle size. Larger surface areas & more accessible adsorption active sites are to blame for this effect, which is produced when particles are made smaller [32].

### Influence of Initial Dye Concentration

The effect of initial BF dye concentration on the adsorption processes of BF and E dyes onto IL and AL were done at the concentration level of 35–335mg/L as shown in Figure 6. Increasing the initial concentration of dye reduces the efficacy of dye removal. This is since dye's repulsive force or steric interference on both the adsorbent & bulk phase may inhibit further adsorption, even if the active sites in the adsorbents necessary for adsorption of the dye molecules are available [9].

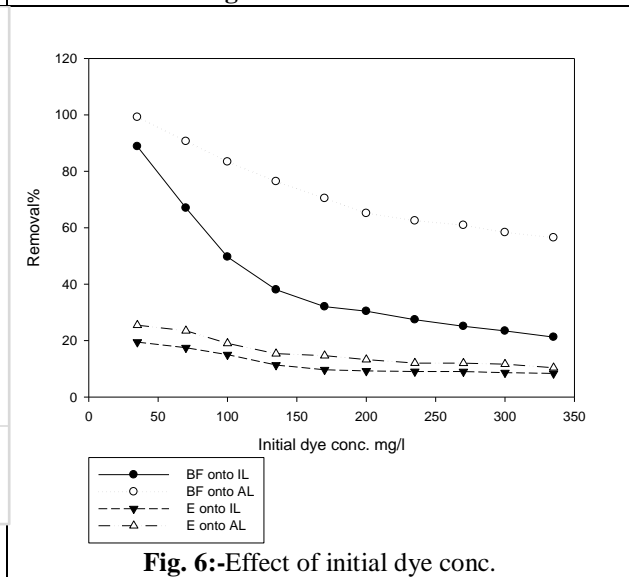
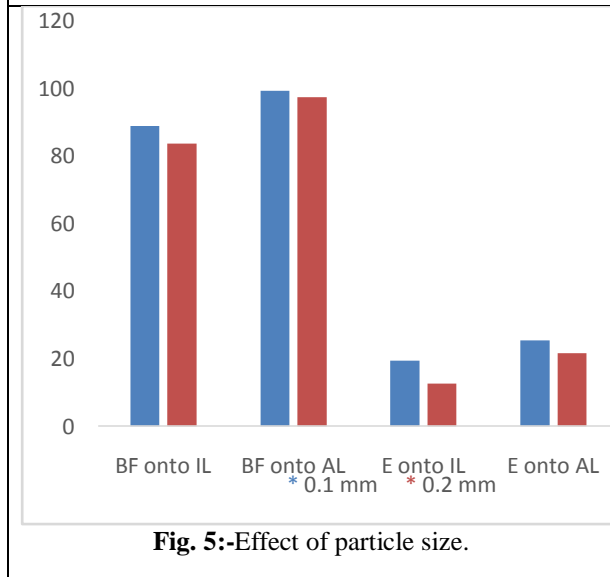
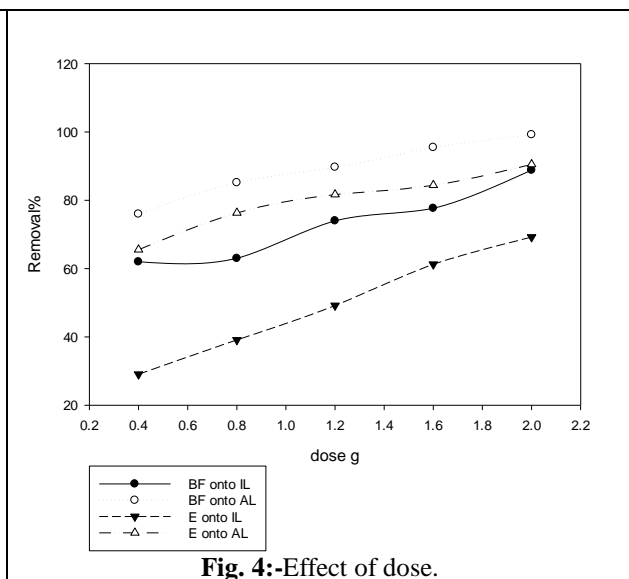
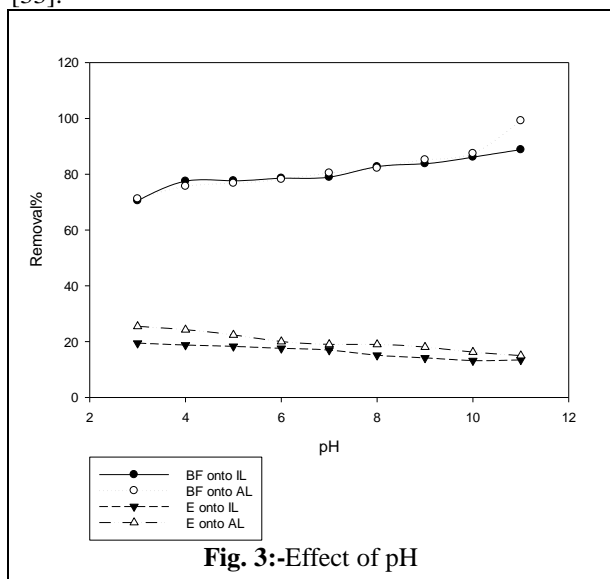
### Influence of Contact Time

The influence of contact time on adsorption processes was investigated over from 5–180 min at optimal  $pH_{11}$  values, initial dye concentration 35 mg/L, adsorbents doses 2g, 0.1mm mesh size of adsorbents and temperature 298K with an agitation speed of 200 rpm. As shown in Figure 9, time at equilibrium was determined to be 30 and 25 min. for BF onto IL & AL respectively, and was found to be 30 and 20 min. for E dye onto IL and AL respectively. Free vacant surface sites of functional groups are responsible for the enhanced dye elimination within the first 30 minutes [9]. After 30 minutes, the removal rate is practically constant either all of the free adsorbing sites have been used up, or because the lasting vacant surface positions are difficult to adsorb because of the repulsion among the dye

molecules on the adsorbents & the bulk phase [9]. Hence, the equilibrium time gained for BF and E dyes adsorptions in this study was about 30 min.

**Influence of Temperature**

The adsorption process is temperature-dependent. The temperature effect was studied at 298 K, 323 K & 343 K at pH<sub>11</sub> for BF, pH<sub>3</sub> for E, initial dye concentration 35mg/L, adsorbents doses 2 g, 0.1mm mesh size of adsorbents & contact time 30 min with agitation speed 200 rpm. Figure 10 shows the deletion of BF and E dyes was increased with rising the temperature from 298 to 343 K. The removal values at 343 K were 92.78, 99.98, 33.76 and 44.31% for BF and E onto IL and AL respectively. Because of temperature's effect on the equilibrium capacity of the adsorbent & the dye molecules' diffusion rate through the outer boundary layer, we can understand this phenomenon [33].





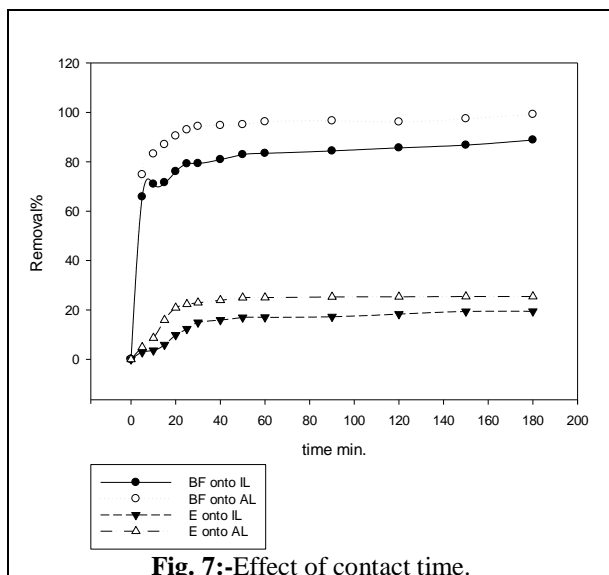


**Fig. 7:-**Effect of contact time.

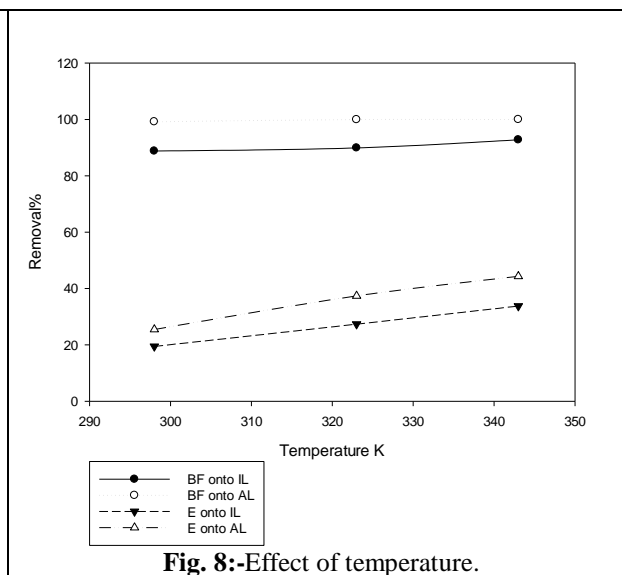


**Fig. 8:-**Effect of temperature.

### Kinetic Study

The kinetic models on the adsorption of BF dye were highlighted using pseudo-1<sup>st</sup> order [34,35], pseudo-2<sup>nd</sup> order [36,37] & intraparticle diffusion [38] as shown in Eqs. (3), (4), and (5) respectively [10].

$$\log (q_e - q_t) = \log (q_e) - k_1 t \quad [3]$$

$$t/q_t = 1/K_2 q_e^2 + t/q_e \quad [4]$$

$$q_t = k_{diff} t^{1/2} + C \quad [5]$$

The sorption capacity of the adsorbent was described by pseudo-2<sup>nd</sup> order kinetics and the diffusion process were represented by pseudo-1<sup>st</sup> order kinetics [39, 40].

### Elovich kinetic model

Adsorption rate calculations on heterogeneous surfaces are accessible to the Elovich kinetic model [41,42]. Elovich extreme adsorption capacity & Elovich constant can be estimated from Eq (6)

$$q_t = (1/\beta) \ln t + (1/\beta) \ln \alpha \beta \quad [6]$$

The values of  $\alpha$  &  $\beta$  can be gained from the slope and the intercept of a straight-line plot of  $q_t$  against  $\ln t$  [43]. According to the data shown in table 2, It was found that the pseudo-second-order kinetics is well-adjusted equated to the pseudo-1<sup>st</sup>-order kinetics and intraparticle diffusion model. A high  $R^2$  values 0.995, 0.9998, 0.964 and 0.989 for adsorption of BF and E onto IL and AL respectively.

The maximum capacities of adsorption  $q_e$  values (1.5610 mg/g, 1.7361 mg/g, 0.4089 mg/g and 0.4827 mg/g in the same sequence) according to pseudo-second-order kinetics. These numbers were larger than those predicted by the pseudo-first-order model, indicating that the pseudo-2<sup>nd</sup>-order kinetics fits the data quite well. Elovich kinetic model was not suggested to use for describing the kinetic process. The  $R^2$  values for the pseudo-1<sup>st</sup>-order and intraparticle diffusion model were relatively low and the calculated  $q_e$  values according to pseudo-1<sup>st</sup>-order kinetics were lower than the experimental  $q_e$  values. As a result, the adsorption onto lupine peel fitted well into the pseudo-2<sup>nd</sup> order kinetic model.

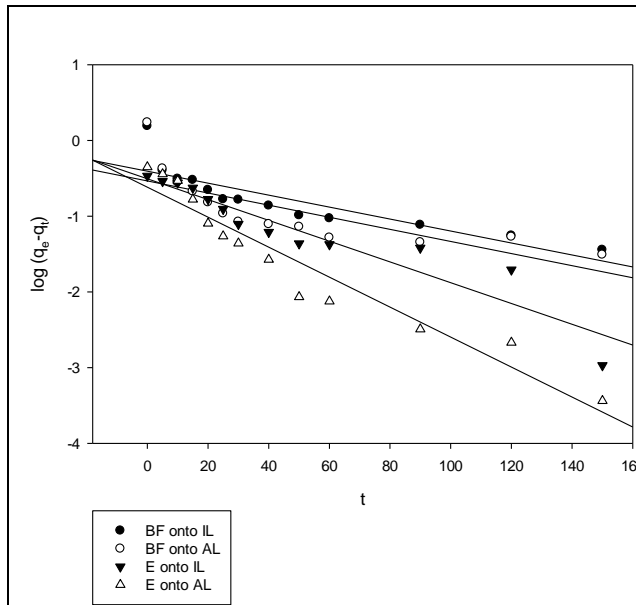


Fig. 9:- First order kinetic model.

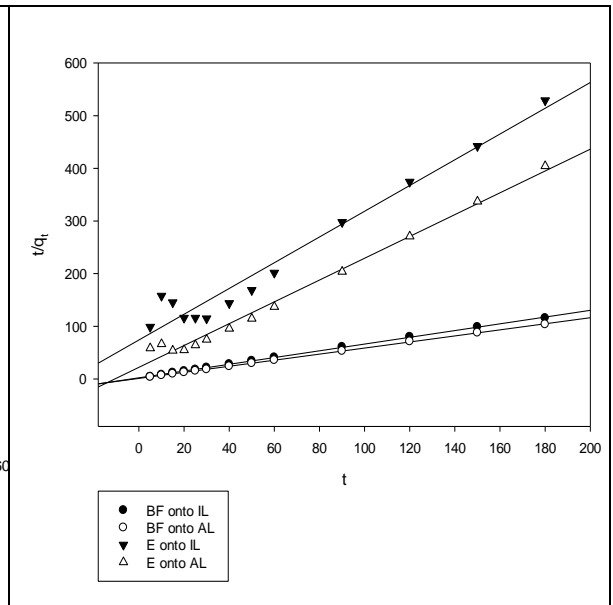


Fig. 10:- Second order kinetic model.

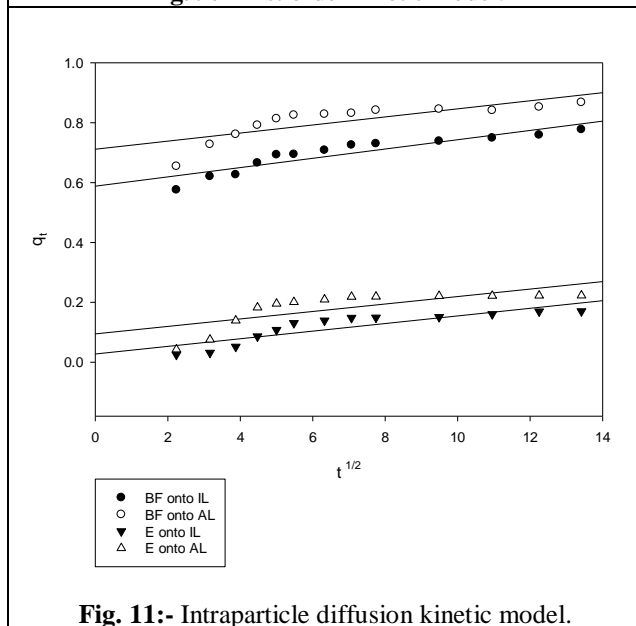


Fig. 11:- Intraparticle diffusion kinetic model.

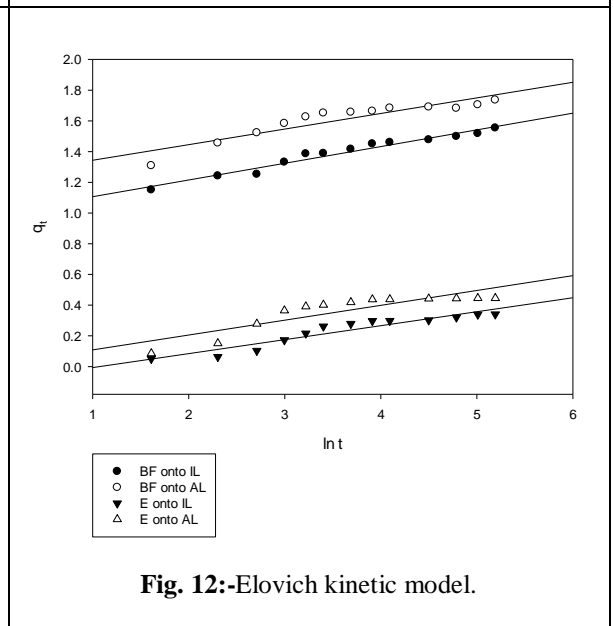


Fig. 12:-Elovich kinetic model.

Table (2):- Kinetic parameters for BF dye adsorption onto IL & AL.

Parameter	BF onto IL	BF onto AL	E onto IL	E onto AL
Pseudo-first order kinetic model				
$K_1$	0.0079	0.0080	0.0137	0.0198
$q_e$	0.6670	0.5865	0.6037	0.5403
$R^2$	0.7555	0.6037	0.8943	0.9294
Pseudo-second order kinetic model				
$K_2$				
$q_e$	0.1833	0.2903	0.0809	0.1938
$R^2$	1.5610	1.7361	0.4089	0.4827
	0.995	0.9998	0.9644	0.9886
Intraparticle diffusion kinetic model				
$K_{id}$				

C	0.0155	0.0135	0.0127	0.0125
R <sup>2</sup>	0.5881	0.7115	0.0274	0.0946
	0.8438	0.6425	0.7598	0.5486
Elovich kinetic model				
$\alpha$	1.0450 x10 <sup>3</sup>	21.0503 x10 <sup>3</sup>	0.0310	0.1092
$\beta$	9.1912	9.8522	11.0011	10.3306
R <sup>2</sup>	0.9622	0.8435	0.9002	0.7672

### Adsorption Isotherms

The Langmuir & Freundlich adsorption isotherms are utilized to describe the adsorbents' surface properties, affinity and sorption process. Monolayer adsorption is assumed here was justified by the Langmuir adsorption isotherm (Figure 13), which states that no adsorption will occur if the adsorbate has already covered all of the active sites [44,45].

The Langmuir adsorption isotherm can be articulated through Eqs. (7)

$$c_e/q_e = c_e/q_m + 1/k_l q_m \quad [7]$$

The separation factor  $R_L$  can be calculated from Eq. (8) which predicts whether the adsorption was favorable or unfavorable in terms of equilibrium parameter or dimensionless constant.

$$R_L = 1/(1 + k_1 C_0) \quad [8]$$

The value of  $R_L$  point to whether the isotherm is unfavorable ( $R_L$  more than 1), linear ( $R_L = 1$ ), favorable ( $R_L$  less than 1), or irreversible ( $R_L = 0$ ). As presented in Table 2, the values of  $R_L$  (among 0 & 1) indicate that the isotherm was favorable [46].

The Freundlich adsorption isotherms explained the multilayer and heterogeneous adsorption on the surface of adsorbate [47,48]. The results were expressed in Figure 14.

Freundlich adsorption isotherm can be articulated through Eqs. (9).

$$\ln q_e = \ln K_f + (1/n) \ln C_e \quad [9]$$

If  $n$  is more than 1, it indicates that the adsorbate is being favorably adsorbed on the adsorbent. The adsorption intensity increases as  $n$  increases [49]. So, the adsorption processes of BF onto IL and AL were well described by Freundlich isotherm model, as the high  $R^2$  values (0.9606 and 0.9677) & the greater  $n$  values indicates stronger the adsorption intensity. While the adsorption processes of E onto IL and AL were well described by Langmuir isotherm model, as the high  $R^2$  values (0.9733 and 0.9866) and low  $R_L$  values. So, the active sites are covered once by the adsorbate and a monolayer was formed.

### Temkin Isotherm

It is assumed in this model that the heat of adsorption of all molecules in the layer will decrease linearly rather than logarithmically with coverage and the model also ignores the extremes of concentration, both small and big [50,51]. The model is given by the following equation (10) [52].

$$q_e = B \ln A_T + B \ln C_e \quad [10] \quad \text{where } B = RT/b_T$$

It can be deduced from Temkin plot shown in figure 17 that, the following values were assessed:  $A_T = 5.6275$  L/g, 5.1701 L/g, 0.0692 L/g and 0.0788 L/g for BF and E dyes adsorption onto IL and AL respectively. It was estimated also, that  $B = 0.2317$  J/mol 0.6001 J/mol, 0.2053 J/mol and 0.2660 J/mol for the adsorption in the same sequence. This points to a physical adsorption process, as indicated by the sorption heat [24].

### Dubinin–Radushkevich isotherm model

This model is frequently employed to characterize the adsorption mechanism on a heterogeneous surface, where the energy is distributed in a Gaussian fashion [53]. Adsorption is modeled as a function of a pore-filling mechanism and the model is based on a semi-empirical equation. It is frequently used to discriminate among chemical and physical adsorption [54]. Many times, the model has been able to provide a good match for data including both high solute activity and a moderate concentration range [9].

$$\ln q_e = \ln q_s - k_{DR} \epsilon^2 \quad [11]$$

$\epsilon$  is Dubinin–Radushkevich isotherm constant which can be calculated from Eq. (12)

$$\epsilon = RT \ln (1 + 1 / c_e) \quad [12]$$

E (for displacing an adsorbate molecule from its position in the sorption space to infinity) can be calculated for each adsorbate molecule using Eq. (13)

$$E = 1 / (2k_{DR})^{1/2} \quad [13]$$

All appropriate information will fit on the same curve (Figure 18), called the characteristic curve, when adsorption data from changed temperatures are plotted as a function of logarithm of amount adsorbed ( $\ln q_e$ ) against  $\epsilon^2$  the square of potential energy [52, 55, 56].

From Dubinin-Radushkevich (D-R) isotherm data, the values of E were 0.5, 2.357, 0.05 and 0.0707 KJ/mol designating a physisorption process [55].

It is clear that the  $R^2$  values for all 4 various adsorption isotherm types are not the same. Table 2 displays correlation coefficient  $R^2$  values that, as they approach 1, indicate which adsorption isotherm model is most suited for BF and E onto IL and AL [51].

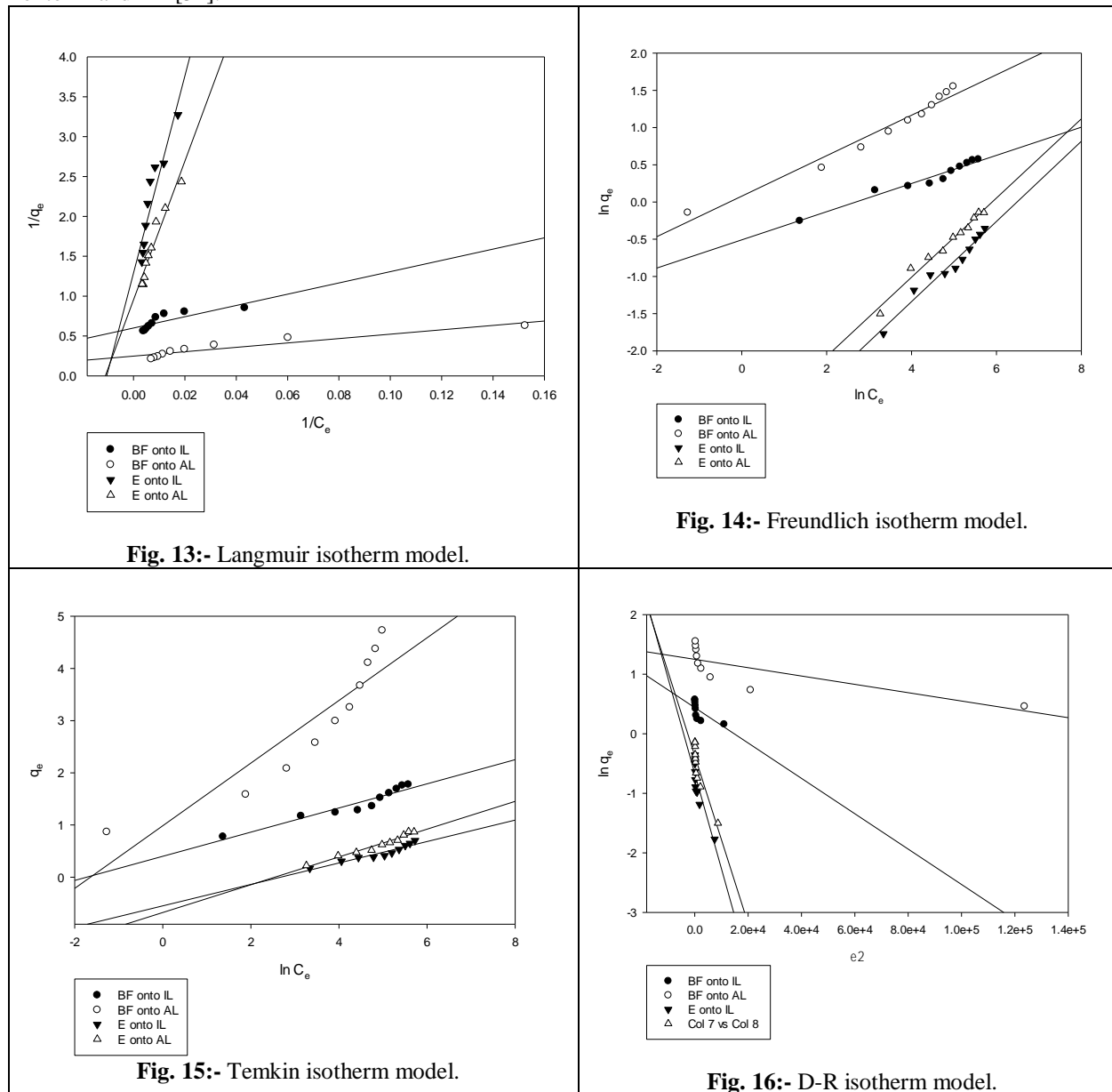


**Table (3):-** Isotherm parameters for BF dye adsorption onto IL & AL.

Parameter	BF onto IL	BF onto AL	E onto IL	E onto AL
Langmuir isotherm model				
b	0.2528	1.4378	0.0097	0.0099
q <sub>o</sub>	1.5344	2.9913	0.7983	1.0921
R <sup>2</sup>	0.8613	0.8259	0.9733	0.9866
R <sub>L</sub> for initial dye concentration				
35	0.1015	0.0195	0.7465	0.7427
70	0.0535	0.0098	0.5956	0.5907
100	0.0381	0.0069	0.5076	0.5025
135	0.0285	0.0051	0.4330	0.4280
170	0.0227	0.0041	0.3775	0.3727
200	0.0194	0.0035	0.3401	0.3356
235	0.0166	0.0030	0.3049	0.3006
270	0.0144	0.0026	0.2763	0.2723
300	0.0130	0.0023	0.2558	0.2519
325	0.0117	0.0021	0.2353	0.2317
Freundlich isotherm model				
K <sub>f</sub>	0.6011	1.0812	1.8574	1.8797
n	5.2798	3.6778	0.0305	0.0434
R <sup>2</sup>	0.9606	0.9677	0.9613	0.9767
Temkin isotherm model				
B	0.2317	0.6001	0.2053	0.2660
A <sub>T</sub>	5.6275	5.1701	0.0692	0.0788
b <sub>T</sub>	10.693 x 10 <sup>3</sup>	4.1286 x 10 <sup>3</sup>	12.0681	9.3142
R <sup>2</sup>	0.9199	0.8315	0.9112	0.9622
Dubinin-Radushkevich (D-R) isotherm model				
K <sub>DR</sub>				
q <sub>s</sub>	2 x 10 <sup>-6</sup>	9 x 10 <sup>-8</sup>	2 x 10 <sup>-4</sup>	1 x 10 <sup>-4</sup>
E	2.4717	13.5425	0.2152	0.4287
R <sup>2</sup>	0.500	2.3570	0.050	0.0707
	0.6679	0.5872	0.7589	0.7980

### Calculation of thermodynamic parameters

To determine the result of temperature on the adsorption of BF on AL and IL, it is important to determine the free energy variation ( $\Delta G^\circ$ ), enthalpy modification ( $\Delta H^\circ$ ) and entropy change ( $\Delta S^\circ$ ). The apparent equilibrium constant ( $K_c$ ) of the adsorption is defined as [57]

$$k_c' = c_{ad,e}/c_e \quad [14]$$

In the lowest experimental BF concentration, the value of  $K_c$  can be determined [56]. Then the change of Gibbs free energy ( $\Delta G^\circ$ ) was determined by substituting the value of  $K_c$  into the following equation.

$$\Delta G^\circ = -RT \ln K_c \quad [15]$$

By applying van't Hoff equation of  $\Delta G^\circ$  vs T, the change of enthalpy ( $\Delta H^\circ$ ) & entropy ( $\Delta S^\circ$ ) can be obtained.

$$\Delta G^\circ = \Delta H^\circ - T \Delta S^\circ \quad [16]$$

Table 3 displays the results of Eq. (15) for the standard Gibbs free energy alteration during the adsorption process. Adsorption of BF onto IL and AL resulted in negative  $\Delta G^\circ$  values because of the spontaneous nature of the adsorption processes & the significant preference of BF onto these two surfaces. As the temperature rises, the spontaneous nature of adsorption of BF reduces, as shown by a drop in the negative value of  $\Delta G^\circ$ , suggesting that the adsorption is enhanced at higher temperatures. Adsorption on the BF/Lemon Peel system was verified to be endothermic thanks to the positive value of  $\Delta H^\circ$ , and the increased unpredictability at the solid-solute interface was validated thanks to the positive values of  $\Delta S^\circ$ . In addition, the low value of  $\Delta S^\circ$  indicated that the entropy does not alter significantly. [58] on the other hand, E adsorption processes onto IL and AL were nonspontaneous and not favorable as the values of  $\Delta G^\circ$  are positive, but endothermic and random as the values of  $\Delta H^\circ$  and  $\Delta S^\circ$  are positive.

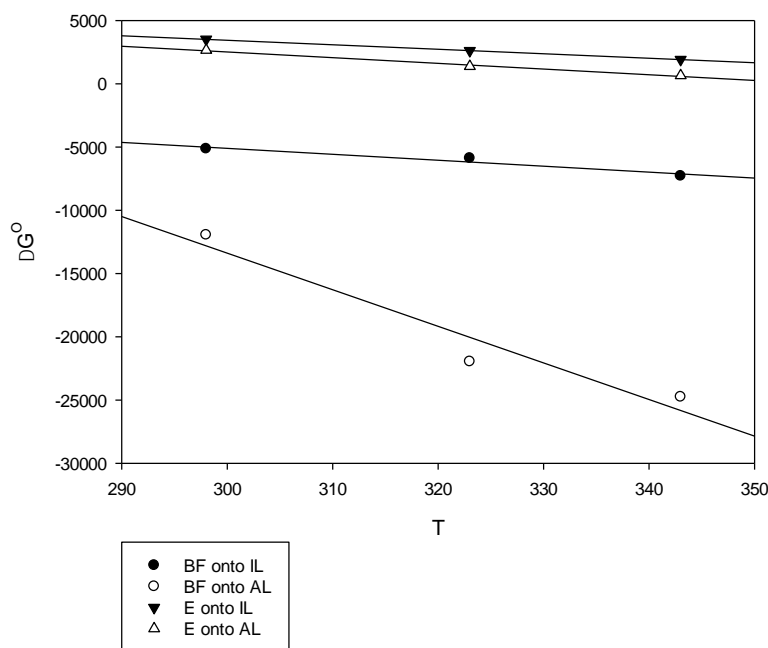


Fig. 17:- Thermodynamic parameters of BF and E adsorption onto IL and AL.

Table (4):- Thermodynamic parameters for BF dye adsorption onto IL & AL.

Parameter	BF onto IL	BF onto AL	E onto IL	E onto AL
$\Delta G^\circ$ at				
298K	-5.1347	-11.9426	3.5217	2.6636
323K	-5.8737	-21.9679	2.6248	1.3878
343K	-7.2815	-24.7515	1.9226	0.6519
$\Delta H^\circ$	8.9937	73.4430	14.113	16.017
$\Delta S^\circ$	0.0469	0.2894	0.0356	0.0450
$R^2$	0.9426	0.9381	1	0.9920

### Conclusion:-

Using of low-cost lupine peel waste for the elimination of Basic Fuchsin and Eosin dyes from aqueous solution was studied in batch experiments. Lupine peel shows a higher adsorption capacity value in the activated form and the adsorption equilibrium was rapid for the adsorption process. Adsorption kinetics could be defined by a rate equation of pseudo-second order. The experimental data most closely followed the Langmuir & Freundlich isotherms, which describe the adsorption processes. By increasing the temperature, both dyes removal increased so the adsorption process was endothermic. An overall higher selectivity for Basic Fuchsin dye than Eosin dye was observed showing that lupine peel can be effectively applied to the expulsion of basic fuchsin from aqueous solutions. As a result, lupine peel was identified as an active & inexpensive adsorbent for the elimination of dyes from dye-containing industrial effluent.

### List of appreviations

$q$ ( $\text{mg.g}^{-1}$ )	the amount of adsorbed dye per g of adsorbent
$C_0$ ( $\text{mg.l}^{-1}$ )	the initial dye concentration
$C_e$ ( $\text{mg.l}^{-1}$ )	the dye concentration at equilibrium
$V$ (l)	the volume of the dye solution
$m$ (g)	the mass of the adsorbent
$q_e$ ( $\text{mg.g}^{-1}$ )	the amount of adsorbed dye per g of adsorbent at equilibrium
$q_t$ ( $\text{mg.g}^{-1}$ )	the amount of adsorbed dye per g of adsorbent at time $t$
$t$ (min)	the time

$k_1$ ( $\text{min}^{-1}$ )	the pseudo-first-order rate constant
$k_2$ ( $\text{g.mg}^{-1}.\text{min}^{-1}$ )	the pseudo-second-order constant
$K_{id}$ ( $\text{mg.g}^{-1}.\text{min}^{-1/2}$ )	the intraparticle diffusion rate constant
$C$ ( $\text{mg.g}^{-1}$ )	a constant that gives an idea about the boundary layer thickness
$\alpha$ ( $\text{mg.g}^{-1}.\text{min}^{-1}$ )	the initial adsorption rate
$\beta$ ( $\text{g.mg}^{-1}$ )	the desorption constant related to the extent of surface coverage and activation energy for chemisorption
$q_m$ ( $\text{mg.g}^{-1}$ )	adsorption efficiency constant
$K_l$	adsorption energy constant
$R_L$	the Langmuir constant
$K_f$ ( $\text{L.g}^{-1}$ )	is the Freundlich constant at bonding energy and distribution
$N$	the heterogeneity factor or adsorption power
$A_T$ ( $\text{l.mg}^{-1}$ )	equilibrium binding constant
$B$	Temkin heat of adsorption constant
$R$ ( $8.314 \text{ J.mol}^{-1}.\text{K}^{-1}$ )	gas constant
$T$ (298 K)	the temperature of the system
$q_s$ ( $\text{mg.g}^{-1}$ )	theoretical isotherm saturation capacity
$K_{DR}$ ( $\text{mol}^2.\text{kJ}^{-2}$ )	Dubinin–Radushkevich isotherm constant
$\epsilon$ ( $\text{kJ} \square \text{mol}^{-1}$ )	the adsorption potential based on the Polanyi's potential theory
$E$ ( $\text{kJ} \square \text{mol}^{-1}$ )	the mean free energy per molecule of adsorbate
$C_{ad,e}$ ( $\text{mg.l}^{-1}$ )	the concentration of adsorbate on the adsorbent at equilibrium
$\Delta G^\circ$ ( $\text{KJ.mol}^{-1}$ )	the change of Gibbs free energy
$\Delta H^\circ$ ( $\text{KJ.mol}^{-1}$ )	the change of enthalpy
$\Delta S^\circ$ ( $\text{KJ.mol}^{-1}$ )	the change of entropy

### References:-

- [1] G. K. Sarma, S. S. Gupta, K. G. Bhattacharyya, Removal of hazardous basic dyes from aqueous solution by adsorption onto kaolinite and acid-treated kaolinite: kinetics, isotherm and mechanistic study. *Journal of Springer Nature Switzerland*. 1:211 (2019). <https://doi.org/10.1007/s42452-019-0216-y>.
- [2] B. Zineb, E. Imane, K. Mohammed, N. Mostafa, N. Isabel, Z. Hicham, Removal of Basic Dyes from Aqueous Solutions by Adsorption onto Moroccan Clay (Fez City), *Mediterranean Journal of Chemistry*. 8(2) (2019) 158-167.
- [3] M. El-Azazy, A. S. El-Shafie, A. Ashraf, A. A. Issa, Eco-Structured Biosorptive Removal of Basic Fuchsin Using Pistachio Nutshells: A Definitive Screening Design—Based Approach. *J. Appl. Sci.* 9 (2019) 4855. doi:10.3390/app9224855.
- [4] E. Mohammadine, Removal of Basic Fuchsin dye from water using mussel shell biomass waste as an adsorbent: Equilibrium, kinetics, and thermodynamics, *Journal of Taibah University for Science*. 10(5) (2018) 664-674.
- [5] B. Aysha, I. Irfan, Z. Hina, G. Ezaz, N. Ammara, B. Awais, R. Sibtain, A. Jahanzaib, H. Sajjad, S. A. Saleh, S. Ramsha, N. Yasra, A. Rizwana, I. Shmaaila, Removal of Eosin dye from simulated media onto lemon peel-based low cost biosorbent. *Arabian Journal of Chemistry*. 15 (2022) 103873.
- [6] K. S. Guruge, P. Goswami, R. Tanoue, K. Nomiyama, R. Wijesekara, T. S. Dharmaratne, First nationwide investigation and environmental risk assessment of 72 pharmaceuticals and personal care products from Sri Lankan surface waterways. *J. Sci. Total Environ.* 690 (2019) 683–695.
- [7] Y. Liu, Y. Che, Y. Shi, D. Wan, J. Chen, S. Xiao, Adsorption of toxic dye Eosin Y from aqueous solution by clay/carbon composite derived from spent bleaching earth. *J. Water Environ. Res.* 93(1) (2021) 159–169.
- [8] A. M. K. Yasser, F. A. Gamal, A. M. Mohamed, Effect of Tryptophan and Ascorbic Acid on Yield and Some Chemical Constituents of Lupine (*Lupinus termis* L.) Plants. *Egypt. J. Agron.* 42(1) (2020) 47- 61.
- [9] A. N. Alene, G. Y. Abate, A. T. Habte, D. M. Getahun, Utilization of a Novel Low-Cost Gibto (*Lupinus Albus*) Seed Peel Waste for the Removal of Malachite Green Dye: Equilibrium, Kinetic, and Thermodynamic Studies. *Hindawi Journal of Chemistry*. (2021) ID 6618510, 16 pages.
- [10] S. Priya, P. D. Jason, R. Sudipta, In situ ATR-FTIR spectroscopy for evidencing the adsorption mechanism of ammonium on a pinewood-derived biochar. *Journal of Agriculture & Environmental Letters*. 8(1) (2023) 20097. <https://doi.org/10.1002/ael2.20097>
- [11] M. Kavisri, A. Marykutty, S. R. N. Karthik, J. Aravindkumar, D. Balaji, S. Ramamoorthy, S. Sivaraj, S. Ramachandran, M. Meivelu, Adsorption isotherm, kinetics and response surface methodology optimization of

cadmium (Cd) removal from aqueous solution by chitosan biopolymers from cephalopod waste. *Journal of Environ Manage.* 22(335) (2023) 117484.

[12] D. Shrestha, Removal of Eosin Y Dye using Activated Carbons from Modified Wood Dust Powder of Dalbergiasisoo. *Journal of Patan Pragya.* 8(1) (2021) 2595-3278.

[13] S. Zuhara, S. Pradhan, Y. Zakaria, A. R. Shetty, G. McKay, Removal of Methylene Blue from Water Using Magnetic GTL-Derived Biosolids: Study of Adsorption Isotherms and Kinetic Models. *Journal of Molecules.* 28(3) (2023) 1511.

[14] C. Yusra, A. H. Muhammad, R. Umer, A. B. Ijaz, A. Hafeez, J. Yasir, A.A. Fahad, A. K. Elham, Effective Removal of Reactive and Direct Dyes from Colored Wastewater Using Low-Cost Novel Bentonite Nanocomposites. *Journal of Water.* 14 (2022) 3604.

<https://doi.org/10.3390/w14223604><https://www.mdpi.com/journal/water>

[15] O. S. Bello, K. A. Adegoke, O. O. Akinyunni, Preparation and characterization of a novel adsorbent from *Moringa oleifera* leaf. *Journal of Applied Water Science.* 7(3) (2017) 1295–1305.

[16] J. Fito, Fluoride removal from aqueous solution onto activated carbon of *Catha edulis* through the adsorption treatment technology. *Journal of Environmental Systems Research.* 8(1) (2019) 25.

[17] N. K. Mondal and S. Kar, Potentiality of banana peel for removal of congo red dye from aqueous solution: isotherm, kinetics and thermodynamics studies. *Journal of Applied Water Science.* 8(6) (2018) 157.

[18] M. T. Uddin, M. A. Rahman, M. Rukanuzzaman, M. A. Islam, A potential low-cost adsorbent for the removal of cationic dyes from aqueous solutions. *Journal of Applied Water Science.* 7(6) (2017) 2831–2842.

[19] A. E. Ismat, K. Marufa, K. M. Afroza, M. Owaleur Rahman, K. M. Anis-Ul-Haque, M. A. Jahangir, Removal of Dye from Wastewater Using a Novel Composite Film Incorporating Nanocellulose. *Journal of Hindawi Advances in Polymer Technology.* 9 (2023) 4431941. <https://doi.org/10.1155/2023/4431941>

[20] V. S. Munagapati, D. S. Kim, Adsorption of anionic azo dye congo red from aqueous solution by cationic modified orange peel powder. *Journal of Molecular Liquids.* 220 (2016) 540–548.

[21] M. A. Ahmad, N. S. Afandi, O. S. Bello, Optimization of process variables by response surface methodology for malachite green dye removal using lime peel activated carbon. *Journal of Applied Water Science.* 7(2) (2017) 717–727.

[22] V. S. Munagapati, V. Yarramuthi, Y. Kim, K. M. Lee, D.-S. Kim, Removal of anionic dyes (reactive black 5 and congo red) from aqueous solutions using banana peel powder as an adsorbent. *Journal of Ecotoxicology and Environmental Safety.* 148 (2018) 601–607.

[23] B. Umair, K. U. Mohammad, M.A. Gondal, Removal of hazardous azo dye from water using synthetic nano adsorbent: Facile synthesis, characterization, adsorption, regeneration and design of experiments. *Journal of Colloids and Surfaces A: Physicochemical and Engineering Aspects.* 584(2) (2020) 124031.

[24] N. A. Rahmat, Removal of remazol brilliant blue R from aqueous solution by adsorption using pineapple leaf powder and lime peel powder. *Journal of Water, Air, & Soil Pollution.* 227(4) (2016) 105.

[25] A. Ishaq, A. H. Muhammad, R. Umer, A. B. Ijaz, A. K. Rais, A. K. Elham, Green Nanocomposite for the Adsorption of Toxic Dyes Removal from Colored Waters. *Journal of Coatings.* 12 (2022) 1955. <https://doi.org/10.3390/coatings12121955><https://www.mdpi.com/journal/coatings>

[26] A. Patel, D. Sharma, P. Kharkar, D. Mehta, Application of activated carbon in waste water treatment, *International Journal of Engineering Applied Sciences and Technology,* 3(12) (2019) ISSN No. 2455-2143, Pages 63-66

[27] A. Hashema, O. A. Chukwunonso, E.S. Abdel-Halim, A. Amr, S. Faraga, A.A. Aly, Instrumental characteristics and acid blue 193 dye sorption properties of novel lupine seed powder, *Cleaner Chemical Engineering* 2 (2022) 100011.

[28] A. Zainab, R. Salih, Y. G. Maryam, Z. A. Shahad, T. A. Zainab, Possibility of Utilizing the Lemon Peels in Removing of Red Reactive (RR) Dye from Simulated Aqueous Solution. *Journal of Green Engineering (JGE).* 10 (2020) 10.

[29] E. C. Lima, H. B. Ahmad, C. M. P. Juan, A. Ioannis, A critical review of the estimation of the thermodynamic parameters on adsorption equilibria. Wrong use of equilibrium constant in the Van't Hoof equation for calculation of thermodynamic parameters of adsorption. *Journal of molecular liquids.* 273 (2019) 425-434.

[30] P. S. Kumara, L. Korvinga, K. J. Keesmana, M. C. M. Loosdrecht, G. Witkamp, Effect of pore size distribution and particle size of porous metal oxides on phosphate adsorption capacity and kinetics. *Journal of Chemical Engineering.* 358 (2019) 160–169.

[31] D. Pathania, S. Sharma, P. Singh, Removal of methylene blue by adsorption onto activated carbon developed from *Ficus carica* bast. *Arabian Journal of Chemistry.* 10(1) (2017) S1445–S1451.



- [32] S. Karaa, C. Aydinera, E. Demirbasb, M. Kobya and N. Dizgea, Modeling the effects of adsorbent dose and particle size on the adsorption of reactive textile dyes by fly ash. *Journal of Desalination* 212 (2007) 282–293.
- [33] F. Raposo, M. A. De La Rubia, R. Borja, Methylene blue number as useful indicator to evaluate the adsorptive capacity of granular activated carbon in batch mode: Influence of adsorbate/adsorbent mass ratio and particle size. *Journal of Hazardous Materials* 165 (2009) 291–299.
- [34] M. Musah, Y. Azeh, J. T. Mathew, M. T. Umar, Z. Abdulhamid, A. I. Muhammad, Adsorption Kinetics and Isotherm Models: A Review. *Caliphate Journal of Science & Technology. CaJoST.* 1 (2022) 20-26.
- [35] S. M. Z. Mohd, A. Muhammad, S. A. Syed, Adsorption Isotherm and Kinetic Study of Methane on Palm Kernel Shell-Derived Activated Carbon. *Journal of Bioresources and Bioproducts.* 8(1) (2023) 66-77
- [36] A. N. Ebelegi, N. Ayawei, D. Wankasi, Interpretation of Adsorption Thermodynamics and Kinetics. *Journal of Physical Chemistry.* 10 (2020) 166-182.
- [37] A. A. Akram, D. Axelle, M. Mohammed, M.B. Anne, M. Nader, CO<sub>2</sub> capture using in-situ polymerized amines into pore-expanded-SBA-15: Performance evaluation, kinetics, and adsorption isotherms. *Journal of Fuel.* 333(1) (2023) 126401. <https://doi.org/10.1016/j.fuel.2022.126401>
- [38] R. A. Lina, P. Le Coustumer, R. G. Stéphane, Z. Stéphane, S. Serge, Removal efficiency and adsorption mechanisms of CeO<sub>2</sub> nanoparticles onto granular activated carbon used in drinking water treatment plants. *Journal of Science of The Total Environment.* 856(2) (2023) 159261. <https://doi.org/10.1016/j.scitotenv.2022.159261>
- [39] V. S. Munagapati, J. Wen, C. Pan, Y. Gutha, J. Wen, G. M. Reddy, Adsorptive removal of anionic dye (Reactive Black 5) from aqueous solution using chemically modified banana peel powder: kinetic, isotherm, thermodynamic, and reusability studies. *International Journal of Phytoremediation.* 22(3) (2020) 267-278.
- [40] S. Hussain, M. Kamran, S. A. Khan, K. Shaheen, Z. Shah, H. Suoe, Q. Khan, S. Abdul Basit, U Waseeq, Y. O. Al-Ghamdi and U. Ghani, Adsorption, kinetics and thermodynamics studies of methyl orange dye sequestration through chitosan composites films. *International Journal of Biological Macromolecules* 168 (2021) 383–394.
- [41] I. Ghosh, S. Kar, T. Chatterjee, N. Bar, S. K. Das, Removal of methylene blue from aqueous solution using *Lathyrus sativus* husk: adsorption study, MPL and ANN modelling. *Journal of Process Safety and Environmental Protection.* 149 (2021) 345-361.
- [42] M. Khnifira, W. Boumya, J. Attarki, A. Mahsoune, M. Abdennouri, M. Sadiq, S. Kaya, N. Barka, Adsorption characteristics of dopamine by activated carbon: Experimental and theoretical approach. *Journal of Molecular Structure.* 1278 (2023) 134964. <https://doi.org/10.1016/j.molstruc.2023.134964>
- [43] K. S. Tong, M. J. Kassim, A. Azraa, Adsorption of copper ion from its aqueous solution by a novel biosorbent *Uncariagambir*: Equilibrium, kinetics, and thermodynamic studies. *Journal of Chemical Engineering.* 170 (2011) 145–153.
- [44] G. K. Rajahmundry, C. Garlapati, P. S. Kumar, R. S. Alwi, N. V. Dai-Viet, Statistical analysis of adsorption isotherm models and its appropriate selection. *Journal of Chemosphere.* 276 (2021) 130176.
- [45] M. Rajabi, S. Keihankhadiv, Suhas. Comparison and interpretation of isotherm models for the adsorption of dyes, proteins, antibiotics, pesticides and heavy metal ions on different nanomaterials and non-nano materials-a comprehensive review. *Journal of Nano struct Chem.* 13 (2023) 43-65. <https://doi.org/10.1007/s40097-022-00509-x>
- [46] S. S. Shah, T. Sharma, B. A. Dar, R. K. Bamezai, Adsorptive removal of methyl orange dye from aqueous solution using populus leaves: Insights from kinetics, thermodynamics and computational studies. *Journal of Environmental Chemistry and Ecotoxicology.* 3 (2021) 172–181.
- [47] A. A. Mohammad, D. A. Da'ana, Guidelines for the use and interpretation of adsorption isotherm models: A review. *Journal of Hazardous Materials.* 393 (2020) 122383.
- [48] H. Qili, L. Rui, H. Liru, L. Hengyuan, P. Xiangjun, A critical review of adsorption isotherm models for aqueous contaminants: Curve characteristics, site energy distribution and common controversies. *Journal of Environmental Management.* 329(1) (2023) 117104.
- [49] C. Estrada, A. Karen, C. Lozano, Felipe, L. Díaz, R. Alejandro, Thermodynamics and Kinetic Studies for the Adsorption Process of Methyl Orange by Magnetic Activated Carbons. *Journal of Bio One Complete.* 14 (2021) 1–11. <https://doi.org/10.1177/11786221211013336>
- [50] K. Alok, S. Sumati, K. Balasubramanian, A review on algal biosorbents for heavy metal remediation with different adsorption isotherm models. *Journal of Environmental Science and Pollution Research.* 30 (2023) 39474–39493. <https://doi.org/10.1007/s11356-023-25710-5>
- [51] C. A. Riyanto, E. Prabalaras, The adsorption kinetics and isotherm of activated carbon from Water Hyacinth Leaves (*Eichhorniacrassipes*) on Co(II). *International Conference on Science and Science Education. Journal of Physics: Conf. Series* 1307 (2019) 012002.

- [52] A. O. Dada, A. P. Olalekan, A. M. Olatunya, O. Dada, Langmuir, Freundlich, Temkin and Dubinin–Radushkevich Isotherms Studies of Equilibrium Sorption of Zn<sup>2+</sup> Unto Phosphoric Acid Modified Rice Husk. IOSR Journal of Applied Chemistry. 3(1) (2012) ISSN: 2278-5736, PP 38-45.
- [53] J. Wang, X. Guo, Adsorption isotherm models: Classification, physical meaning, application and solving method. Journal of Chemosphere. 258 (2020) 127279.
- [54] P. Chidamparam, M. J. Rajamani, M. Jayabalakrishnan, P. Mohan, B. Govindaraj, L. Arunachalam, S. Selvakumar, Z. J. Joseph, Cellulose-based hydrogel for adsorptive removal of cationic dyes from aqueous solution: isotherms and kinetics. Journal of RSC Advances. 7 (2023) Issue in Progress
- [55] N. Ayawei, A. N. Ebelegi, D. Wankasi, Modelling and Interpretation of Adsorption Isotherms, Hindawi Journal of Chemistry. 2017, Article ID 3039817, 11 pages.
- [56] T. Chen, T. Da, Y. Ma, Reasonable calculation of the thermodynamic parameters from adsorption equilibrium constant. Journal of Molecular Liquids 322 (2021) 114980.
- [57] R. Hana, J. Zhanga, P. Hana, Y. Wanga, Z. Zhaob, M. Tanga, Study of equilibrium, kinetic and thermodynamic parameters about methylene blue adsorption onto natural zeolite, Chemical Engineering Journal, 145 (2009) 496–504.
- [58] M. N. Sahmoune, Evaluation of thermodynamic parameters for adsorption of heavy metals by green adsorbents. Journal of Environmental Chemistry Letters. 17 (2019) 697–704.